Development and validation of an in-line NIR spectroscopic method for continuous blend potency determination in the feed frame of a tablet press.

Fien De Leersnyder[a], Elisabeth Peeters[b], Hasna Djalabi[a], Valérie Vanhoorne[c], Bernd Van Snick[c], Ke Hong[d], Stephen Hammond[e], Angela Yang Liu[b] , Eric Ziemons[f], Chris Vervaet[c], Thomas De Beer[a].

a Laboratory Process Analytical Technology, Department of Pharmaceutics, Ghent University, Ottergemsesteenweg 460, 9000 Ghent, Belgium
b SPECTech Group, Analytical R&D, Worldwide Research and Development, Pfizer Inc., 280 Shennecossett Rd, Groton, USA.
c Laboratory of Pharmaceutical Technology, Department of Pharmaceutics, Ghent University, Ottergemsesteenweg 460, 9000 Ghent, Belgium
d Advanced Manufacturing Technology Group, Pfizer Global Supply, Pfizer Inc., 100 US-206, Peapack, USA.
e Process Analytical Sciences Group, Pfizer Global Supply, Pfizer Inc., 100 US-206, Peapack, USA.
f CIRM, Laboratory of Analytical Chemistry, Department of Pharmacy, University of Liege (ULg), 1 Avenue de l'Hôpital, B36, 4000 Liège, Belgium

Corresponding author: Thomas De Beer, Thomas.debeer@ugent.be, Laboratory of Pharmaceutical Process Analytical Technology, Ottergemsesteenweg 460, Ghent University, Ghent, Belgium.

Abstract:

A calibration model for in-line API quantification based on near infrared (NIR) spectra collection during tableting in the tablet press feed frame was developed and validated. First, the measurement set-up was optimised and the effect of filling degree of the feed frame on the NIR spectra was investigated. Secondly, a predictive API quantification model was developed and validated by calculating the accuracy profile based on the analysis results of validation experiments. Furthermore, based on the data of the accuracy profile, the measurement uncertainty was determined. Finally, the robustness of the API quantification model was evaluated.

An NIR probe (SentroPAT FO) was implemented into the feed frame of a rotary tablet press (Modul™ P) to monitor physical mixtures of a model API (sodium saccharine) and excipients with two different API target concentrations: 5 and 20% (w/w). Cutting notches into the paddle wheel fingers did avoid disturbances of the NIR signal caused by the rotating paddle wheel fingers and hence allowed better and more complete feed frame monitoring. The effect of the design of the notched paddle wheel fingers was also investigated and elucidated that straight paddle wheel fingers did cause less variation

in NIR signal compared to curved paddle wheel fingers. The filling degree of the feed frame was reflected in the raw NIR spectra. Several different calibration models for the prediction of the API content were developed, based on the use of single spectra or averaged spectra, and using partial least squares (PLS) regression or ratio models. These predictive models were then evaluated and validated by processing physical mixtures with different API concentrations not used in the calibration models (validation set). The β-expectation tolerance intervals were calculated for each model and for each of the validated API concentration levels (β was set at 95%). PLS models showed the best predictive performance. For each examined saccharine concentration range (i.e., between 4.5 and 6.5% and between 15 and 25%), at least 95% of future measurements will not deviate more than 15% from the true value.

Keywords

Process Analytical Technology, In-line NIR spectroscopy, Rotary tablet press, Feed frame, Partial Least Squares, Accuracy profiles

Abbreviations

0-0	Original paddle wheel without notches
1-10 / 2-16	Paddle wheel with notches of 1 mm deep and 10 mm wide/2 mm deep and 16 mm wide
3-30	Customized paddle wheel of GEA Pharma systems with a notch of 3 mm deep and 30 mm wide
A%	Absorbance ratio
MCC	Microcystalline cellulose
MLR	Multiple linear regression
MSC	Multiplicative scatter correction
NIR(S)	Near infrared (spectroscopy)

PAT	Process analytical technology
PCA	Principal components analysis
PLS	Partial least squares
RMSE(P)	Root mean square error (of prediction)
rpm	Rotations per minute
RTR(t)	Real time release (testing)
SFSTP	Société Française des Sciences et Techniques Pharmaceutiques
SNV	Standard normal variate
stdev	Standard deviation
tpm	Tablets per minute

45

1. Introduction

Tablets are worldwide the most important solid drug dosage forms. Tablets are generally produced in rotary tablet presses, enabling continuous tablet production [1]. A key to successful continuous processing is the implementation of real-time release testing (RTRt) and real-time release (RTR). RTRt is based on a firm understanding of the process and the relationship between process parameters, material attributes and product quality attributes [2]. Process analytical technology (PAT) is to be used for the real-time analysis and control of the manufacturing process [3].

The applicability of near infrared spectroscopy (NIRS) as PAT tool for the off-line and at-/on-/in-line, non-destructive and non-invasive, quantitative and qualitative analysis of tablets has been evaluated numerously [4–8]. NIRS provides information about both physical (e.g. particle size, density) and chemical characteristics (e.g. API content) of the observed material (intermediate and end products) [9,10]. In these studies [4-8], tablets were sampled and manually measured off-line or the tablets were transported to a tablet holder [8] or conveyer belt [11] for automatic off-line/at-line NIR spectral acquisition. To allow RTR of tablets, in-line PAT tools are necessary to assure end-quality of the produced tablets (avoiding a lag time between the moment of tablet production and tablet analysis).

Studies were performed on the in-line quantification of drug and excipient concentrations in tablets directly after compression [9,12]. The aim was to measure all individual tablets, therefore the probe was positioned in such a way that it measured the tablets at the ejection area [9] or directly after ejection [12]. Measuring all individual tablets limited the maximum tablet production speed to the maximal acquisition rate of the NIR spectrometer (80 spectra per second corresponding to 4800 tablets per minute).

A few studies were published in which the final blend circulating in the feed frame of the press was monitored by NIRS [1,3,13,14]. Monitoring blend potency in the feed frame enables the ability for feedback (e.g. to the feeders of the tablet press) or feedforward (e.g. gating tablets to the waste)

control which is important for RTR in continuous manufacturing. Mateo-Ortiz et al. [1] investigated the die filling process and powder flow in-line inside the feed frame through a sapphire window. This paper focused on the flow behaviour inside the feed frame and only briefly discussed API concentration monitoring of the circulating blend. The performance of the quantification models for API concentration monitoring was evaluated by root mean square error (RMSE) values. No model validation was performed.

Liu et al. observed disturbances in the NIR signal, when directly measured inside the feed frame, caused by the rotating paddle wheel of the feed frame in a tablet press [13]. In contrast to Liu et al., Wahl et al. and Ward et al. performed similar experiments on monitoring of blend potency (inside the powder bed of the feed frame) but did not report disturbances caused by the moving paddle wheels [3,13,14]. This could possibly be attributed to different spectrometer measurement parameters (number of scans, integration time, averaging) that impact the spectral quality.

Spectral pre-processing or (mathematical) averaging is always used in the above mentioned studies to extract the desired information (e.g. blend composition) from interacting effects (e.g. non-specific scatter of the sample surface or variable path length through the sample). However, this can also cause the deletion of important physical information (e.g. particle size and density information [15]) about the powder blend inside the feed frame. Since information about powder density and particle size can be very important to understand and optimise the tableting process, the use of spectral pre-processing techniques should be carefully evaluated .

In contrast, in the current study a new approach was used for in-line measurements inside the feed frame of a tablet press. The design of the paddle wheel was adapted, by cutting notches having a well-considered size into the paddle wheel fingers to avoid the spectral disturbances caused by the paddle wheel fingers. Using this set-up, the acquired spectra can be used without pre-processing or filtering. This is essential when physical characteristics (density, particle size) are of interest to be determined in-line, since NIR spectra contain physical information of the material and applying spectral filters on

the data will lead to loss of information [1]. Moreover these filters can be complex in cases when the illumination spot of the probe is partly sampling processed material and partly sampling the paddle finger of the rotating paddle wheel. In this study, raw spectra (without pre-processing or averaging) were evaluated to understand the effect of the filling degree of the feed frame upon the collected NIR spectra.

After optimisation of the measurement set-up, an optimisation design was performed to determine the ideal process settings for the development of an API quantification model. Subsequently, a model for continuous API concentration monitoring in the feed frame of the tablet press via NIRS was developed and validated. For the development of a model for concentration quantification, no mathematical filters and a minimum of spectral pre-processing were necessary, due to the optimised measurement set-up. The developed blend potency determination model was evaluated and validated using the approach introduced by the Société Française des Sciences et Techniques Pharmaceutiques (SFSTP)[16–18] based on accuracy profiles.

The effect of process parameters (tableting speed, paddle speed, paddle type) on the predictive performance of the developed model was also shortly evaluated.

2. Material and methods

2.1. Materials

Test formulations (physical mixtures) consisting of sodium saccharine (JMC corporation, Ulsan, South Korea), microcrystalline cellulose (MCC) (Avicel® PH-102, FMC biopolymer, Cork, Ireland) and lactose (Fast Flo 316, Foremost, Wisconsin, USA) were tableted during the in-line NIR monitoring experiments. Sodium starch glycolate (JRS Pharma, Budenheim, Germany) and magnesium stearate (Mallinckrodt, Dublin, Ireland) were added as disintegrant and lubricant, respectively. The quantitative composition of the processed formulations is shown in Table 1.

The mixture was first blended without lubricant in a three-dimensional mixer (Inversina, Bioengineering AG, Wald, Switzerland) during ten minutes at 25 rotations per minute (rpm). Magnesium stearate was then added and blended for an additional five minutes at 12 rpm, hence avoiding overlubrication. Unless stated otherwise, the formulation with 20% (w/w) sodium saccharine was used throughout the study to perform the experiments. The amount of sodium saccharine, MCC and lactose was varied during the experiments for API monitoring (see further, Table 2). Tableting

2.2. Tableting

Tableting experiments were performed using an industrial high speed rotary tablet press, Modul™P (GEA Pharma Systems – GEA Process Engineering, Halle, Belgium) equipped with ten 8 mm circular flat faced punches and a feed frame with two paddles (as shown in Figure 1a). Paddle wheel 1 had eight fingers, transporting powder towards the overfilling station, while paddle wheel 2 had 12 fingers and was located at the filling station to recover excess powder ejected from the die after weight adjustment. The design of this feed frame has been described elaborately by Peeters et al. [19].

Two versions of paddle wheel 1, were used in this study and will be described in “2.5.1 The effect of notches in the paddle wheel fingers”.

All preblends were compressed to a constant tablet weight of 300 mg with a main compression force of 15 kN. Tableting speed and paddle speeds varied according to the experimental design, but unless

136 stated otherwise a tableting speed of 50 rpm, resulting in 500 tablets per minute (tpm), and a speed
137 of 60 and 85 rpm for paddle 1 and paddle 2 respectively were used.

138 *2.3. NIR spectroscopy*

139 The NIR spectra were collected in reflection mode with a diode array spectrometer:
140 SentroPAT FO (Sentronic, Dresden, Germany). Spectra were acquired at a speed of 15 spectra per
141 second. A spectral range of 1150-2200 nm was covered with a spectral resolution of 2 nm. A
142 SentroProbe DL RS NIR (Sentronic, Dresden, Germany) with a probe length of 185 mm and a diameter
143 of 19 mm, connected to the SentroPAT system via a fibre-optic cable was mounted in the feed frame
144 at a predefined position in very close proximity to the die filling station, thus monitoring the powder
145 blend just before die filling and hence compression (Figure 1a). A customized probe-holding device
146 equipped with a micrometer was used to ensure a firm and steady fixation of the probe through an
147 opening in the top plate of the feed frame and to ensure a reproducible probe depth position (i.e.
148 distance between probe and paddle wheel) (Figure 1b). NIR spectral acquisition started after one
149 minute of tableting to ensure complete filling of the feed frame. The spectral acquisition lasted 7
150 seconds, corresponding to approximately 100 spectra. During the study of the effect of filling degree
151 of the feed frame on the NIR spectra, spectral acquisition started together with tableting.

152 *2.4. Data analysis software*

153 For the development of the API quantification model, SIMCA (Version 13.0.3, Umetrics, Umeå,
154 Sweden) software was used for standard normal variate pre-processing (SNV), Savitzky-Golay
155 smoothing, principal components analysis (PCA) and partial least squares analysis (PLS). Since API
156 concentration is a chemical characteristic, SNV preprocessing could be applied without loss of
157 information. Experimental designs were developed and analysed with MODDE 10 software (Umetrics,
158 Umeå, Sweden) by means of multiple linear regression (MLR). The e.noval software V3.0 (Arlenda,
159 Liège, Belgium) was used to compute all validation results, accuracy, precision, linearity and β-
160 expectation intervals and to build the accuracy profiles.

2.5. Optimisation of measurement set-up for in-line NIR monitoring

2.5.1 The effect of notches in the paddle wheel fingers

In a first step to optimise the measurement set-up, the disturbances in NIR spectra caused by the paddle wheel fingers rotating underneath the probe needed to be eliminated. The originally supplied paddle wheel had eight curved fingers (Figure 2a).

At the position where the paddle wheel fingers pass the NIR probe, notches were sequentially cut out of the eight paddle wheel fingers to investigate whether this adjustment would decrease the spectral disturbances (Figure 2c). Starting with the intact original paddle wheel with eight curved fingers without notches (0-0), the first notch was cut with a depth of 1 mm deep and a width of 10 mm (1-10). The second notch was 1 mm deep and 16 mm wide (1-16), while the third one was 2 mm deep and 16 mm wide (2-16). The difference in notch size was made to investigate the effect of the notch dimensions on the disturbances caused by the fingers. Furthermore, a customized paddle wheel for in-line NIR monitoring with eight straight fingers was offered by GEA Pharma Systems (GEA Process Engineering, Halle, Belgium). This design has a notch of 3 mm deep and 30 mm wide in the middle of each paddle wheel finger (Figure 2b) and was further referred to as “3-30”, in accordance to the dimensions of its notches.

The probe was inserted as low as possible inside the feed frame, ensuring a minimal clearance (0.4 mm) between the probe surface and the paddle wheel fingers. This position was defined as the “base position” of the probe, being the lowest position possible to insert the probe inside the feed frame, without touching the paddle wheel fingers (Figure 3).

The disturbances caused by the paddle wheel fingers moving underneath the NIR probe could be observed in the raw spectra and by PCA analysis. To observe the effect of the rotating paddle wheel fingers on the NIR signal, the variation in absorbance at one wavelength, not influenced by API concentration fluctuations (e.g. 1300 nm) was plotted in function of time and analysed for the possible presence of trends caused by the rotating paddle wheel. The disturbing effect of the rotating paddle

wheel in the NIR spectra could be observed as an increase of absorbance at each wavelength of the spectral range. 1300 nm was chosen in this study to ensure that API concentration variations were excluded.

2.5.2 The influence of paddle type, paddle speed and probe depth

The influence of paddle type, paddle speed and probe depth on the quality of the NIR spectra was investigated by means of an experimental design. Only the notched paddles 2-16 (curved) and 3-30 (straight) were studied. When the 3-30 paddle wheel was used and the probe was positioned at the "base position", the probe was located relatively deeper inside the feed frame compared to when the 2-16 paddle wheel was used (Figure 3b versus c). As the width of the notch of paddle 3-30 was 30 mm, the probe could be inserted deeper into the feed frame (Figure 3c).

Since the probe could not be inserted into the notch of the 2-16 paddle and since the distance between the paddle wheel fingers and the upper plate of the feed frame did not allow an increase of the distance between the probe and the paddle wheel fingers, it was only possible to run experiments at one probe height when the 2-16 paddle was used: the base position. This corresponded to a distance-to-finger of 2 mm.

Two full factorial experimental designs were performed (one for each paddle type) to study the influence of paddle speed and probe depth (only when 3-30 was used) on the quality of the NIR spectra (Supplementary Information: Table 1 and Table 2). The speed of paddle wheel 1 was varied from 10 to 110 rpm, and the speed of paddle wheel 2 was varied from 20 to 140 rpm (using fixed combinations between paddle 1 and 2). The two paddles were compared by analysing the experiments performed with identical settings (probe depth of 2 mm).

The main variation between the spectra of blends with different API concentration must be caused by actual concentration changes and as little as possible by physical characteristics (caused by the circulating wheel). The influence of process and measurement set-up parameters on the spectral variance during one experiment (constant concentration of API) was investigated. The quality of the

NIR spectra was judged by the standard deviation (stdev) between the measured absorbance at four different wavelengths (during one experimental run, including 400 spectra). Wavelengths at specific and selective peaks for lactose and saccharine were selected to analyse since these will be used in the development of the quantitative models. During tableting of blends with an identical API concentration (i.e. identical lactose and saccharine concentration), variance at these wavelengths should be as low as possible, since no concentration difference occurs. This variance will contribute to the model error of the developed models for API concentration quantification. The standard deviation on the absorbance was calculated at different wavelengths: one wavelength that was not influenced by concentration fluctuations: 1300 nm, two lactose-selective wavelengths: 1530 and 1586 nm and one wavelength selective for sodium saccharine: 1664 nm. The stdev of the four wavelengths were analysed as responses of the DoE.

2.5.3 Effect of filling degree on the NIR spectra

It was investigated whether filling of the feed frame could be monitored by in-line NIR during tableting. In this experiment, spectra were acquired during filling (start-up phase) of an empty and cleaned feed frame. The formulation was tableted using paddle wheel 2-16. Since filling degree is expected to be reflected as baseline shifts in the NIR spectra, no pre-processing was applied on the acquired spectra. The raw spectra were plotted and possible trends in the spectra correlated with an increase in filling degree of the feed frame during the start-up phase were analysed.

2.6. Development and validation of in-line NIR model for API content monitoring

Using the optimised measurement set-up, different calibration models were developed for two formulations with target concentrations of 5% and 20% (w/w) sodium saccharine (compensated by MCC/lactose in a ratio 1:2). 20 preblends (Table 2) were prepared with different concentrations of sodium saccharine. For each target concentration, five blends, having different API concentration around this target, were used for calibration of the NIR model and five were used for validation of the developed models. The validation blends had different concentrations compared to the calibration

blends. Calibration and validation spectra were acquired during the processing of these different preblends.

Each blend was fed to the tablet press and the acquisition of spectra over a period of 7 seconds (corresponding to approximately 100 spectra) started after 1 minute of tableting. This was repeated three times per concentration and on three different days. In total, 180 series of spectra, nine per blend, were hence gained.

PCA was used to detect and exclude possible outliers in the spectral data (spectral acquisition that was started before rotation was started, powder lumps…). Calibration models were generated after different pre-processing techniques were applied on the spectra (SNV, multiplicative scatter correction (MSC), second derivatives) and different spectral ranges were evaluated to develop the calibration models. Because of the notches, the use of mathematical filters to select and delete by fingers disturbed spectra was unnecessary. However, since NIR spectra were acquired in a dynamic environment, scatter effects could occur and cause baseline shifts in the NIR signals. Since API concentration is a chemical and not a physical characteristic, pre-processing could be applied on the spectra to remove these unwanted effects, without risk of (chemical) information loss. The models were used to predict the API concentrations of the validation sets based on the acquired spectra. The predicted concentrations were compared to the real (known) concentrations and the root mean square error of prediction (RMSEP) was calculated according to equation 1, to evaluate the model performances.

$$RMSEP = \sqrt{\frac{\sum(x_i - \mu_i)^2}{n}} \quad (1)$$

With x_i: predicted concentration (%)
μ_i: real concentration (%)
n: number of samples

Two approaches were used for the development of calibration models: PLS models and ratio models.

2.6.1 PLS MODELS

For the 5% (w/w) target concentration model, prior to modelling, SNV pre-processing was applied, removing scattering caused by the powder wave behaviour inside the feed frame, on a specific spectral range of 1640-2064 nm. For the 20% (w/w) model, the best models were acquired using spectra on which, prior to modelling, SNV pre-processing and Savitsky-Golay (eliminating noise in the spectra) smoothing (15 points) was applied on a specific spectral range of 1646-2022 nm.

Two PLS models were built for each target concentration. Model 1 was built by regressing the 4500 in-line collected and pre-processed spectra (5 concentration levels, 3 repetitions per concentration level per day, 3 days, 100 spectra per repetition) against the true saccharine concentration values. Model 2 was not based on the original single in-line corrected spectra, but on the average of 15 consecutive recorded spectra. 270 pre-processed spectra (5 concentration levels, 3 repetitions per concentration level per day, 3 days, 6 mean spectra per repetition) were used to build this model.

For the development of the PLS models (model 1 and 2), all in-line collected NIR spectra were regressed against the (known) true saccharine concentration. The number of PLS components was chosen, based on the goodness-of-prediction (Q^2 value being the fraction of the total variation of X or Y that can be predicted by a component, as estimated by cross-validation in which cross-validation groups were defined by concentration level). Extra components were added until the goodness-of-prediction did not improve significantly (1 and 2 for models 1 and 2 respectively).

The FDA guideline “Development and Submission of Near Infrared Analytical Procedures” [20] suggests that for blend uniformity analysis, the effective sample size should be comparable to a unit dose. An estimation of the effective sample size was made and set on 29 mg per spectrum. The NIR probe has a spot size of 6 mm, the penetration depth was assumed to be not bigger than 1 mm [11]. The average of 15 spectra thus had an effective sample size of not more than 435 mg, which was in the same size order of the unit dose (i.e. a single tablet).

2.6.2 RATIO MODELS

For each target concentration, two other models (model 3 and model 4) were built by linear regression of the absorbance ratio (A%) against the known (based on weighed masses) saccharine/lactose concentration ratio. A% was calculated using equation 2.

$$A\% = \frac{A_{Sach} - A_{BL}}{A_{Lact} - A_{BL}} \quad (2)$$

In this equation the baseline-correction point A_{BL} was the absorbance at 1300 nm, because neither saccharine, lactose or MCC displayed noticeable absorption at this wavelength, A_{lact} was the absorbance at 1532 nm (i.e. wavelength selective for lactose) and A_{sach} was the absorbance at the saccharine selective wavelengths 1664 nm and 1994 nm for model 3 and 4, respectively. The numerator of equation 2 was thus the baseline-corrected absorbance of the saccharine peak and the denominator is the equivalently calculated baseline-corrected absorbance at 1532 nm, where a lactose peak was located.

2.6.3 VALIDATION OF THE IN-LINE CALIBRATION METHOD

To evaluate the predictive performance of the models, the validation sets were used, one for 5% and one for 20% (w/w) target API concentration.

RMSEP is an indication of the quantitative performance of the developed method, but does not evaluate the risk that every future measurement will be close enough to the unknown true value of the sample [21,22]. SFSTP introduced a strategy for the harmonisation of approaches for the validation of a quantitative analytical procedure [16–18,23]. The strategy is based on the fact that the total error of a measurement is the sum of a systematic error (true bias) and a random error (true variance)[17,21,24–27]. This strategy uses accuracy profiles as a comprehensive measure of the method performance.

The ultimate aim of the validation is to guarantee that the difference (i.e. the total error) between the future measurements (x_i) and their real value (μ_i) will, with a certain probability (β), be lower than a predefined acceptance limit (λ)(equation 3)[17].

$$\Pr\left(|x_i - \mu_i| < \lambda\right) > \beta \tag{3}$$

Validation standards represent the future samples that the method will have to quantify. In this study, the concentration of the validation samples was predicted by means of the four developed models. Based on the predicted values, precision, accuracy and total error of the measurements were calculated. For each concentration level, a two-sided 95% β-expectation tolerance limit was calculated which signifies that 95% of the future measurements will fall between these limits [25,28]. Based on these intervals, the proportion of observations that will fall within the predefined bias acceptance limits -λ and +λ could be determined. The tolerance limits were connected and together with the acceptance limits, the accuracy profile was constructed. As long as the β-expectation interval was included between the predefined acceptance limits, the procedure was guaranteed acceptable [24]. When the β-expectation tolerance interval limits for the considered concentration levels of the validation standards fell within the bias acceptance limits, the upper and lower concentrations of the validation standards defined the upper and lower quantification limits [27]. If the tolerance intervals intersected with the acceptance intervals, the upper and lower quantification limits were defined by the intersection points.

In this study, the accuracy profiles were applied to evaluate the predictive performance of the models. Herewith, the acceptance limits were set at 5, 10 and 15% .

2.7. Effect of paddle type, paddle speed and tableting speed on predictive performance

In this final part of the study, it was investigated if changes in the optimal measurement set-up and applied process settings changed the predictive capability of the best ratio and PLS model. Sequentially, the stdev and RMSEP values of these predictions were calculated, compared and

evaluated. A preblend with a saccharine concentration of 20% (w/w) was tableted to study the effect of paddle type, paddle speed and tableting speed on the predictive performance of the developed calibration models (Table 3).

3. Results and Discussion

3.1. Optimisation of measurement set-up for in-line monitoring.

3.1.1 The effect of notches in the paddle wheel fingers

When spectra were acquired during tableting with the original paddle wheel (0-0), disturbances could be clearly noticed in the raw spectra (Figure 4). An overall increase of the baseline could be observed, with a slightly higher increase at lower wavelengths compared to the higher wavelengths.

In this study, the disturbances in absorbance at one wavelength (at 1300 nm), not influenced by concentration fluctuations, were compared for different paddle types (differing in the dimensions of their notches). In the 0-0 runs (i.e. original paddle without notches), spectral disturbances were seen at a frequency corresponding to the paddle speed, caused by the passing paddle wheel fingers (Figure 4). A similar observation was reported by Liu et al.[13]. Cutting notches into the paddle wheel fingers (1-10, 1-16 and 2-16) was beneficial for the spectral quality of the NIR data acquired in the feed frame. Disturbances, corresponding to the rotating paddle wheel fingers, were not detected anymore. The spectral quality was hence not influenced by the dimension of the evaluated notches (Figure 4).

3.1.2 The influence of paddle type, paddle speed and probe depth upon spectral quality

Both experimental designs (Supplementary Information: Table 1 and Table 2) were analysed separately (2-16 paddle and 3-30 paddle) and analysed as one design (i.e., all experiments with distance-to-finger of 2 mm). In Figure 5, the effect plots for the four responses (stdev on different examined wavelengths being 1300, 1530, 1586 and 1664 nm) are shown, when both experimental designs were combined and analysed as a single design. The effects can be read as the change in response when the factor is

varied between the minimal and maximal setting, keeping all other factors constant. The 95% confidence intervals indicate the uncertainty of the effects.

It could be noticed that the effects on stdev were small, but still significant. The stdev variability between the different experiments (0.00012-0.0050) was larger than the stdev variability of the replicates (0.0012-0.0026).

Paddle speed had no significant effect on the stdev at the different wavelengths. In contrast, a significant effect was attributed to paddle type. When paddle 2-16 was used, the stdev value increased. Therefore, paddle configuration 3-30 was preferred for the development of in-line API monitoring models. The smaller variability at the different examined wavelengths when using paddle 3-30 could be attributed to the fact that the volume of the notch in paddle 3-30 which was almost three times larger (450 mm^3 vs 160 mm^3) creating a more stable powder bed underneath the probe compared to processing with paddle 2-16.

To be able to evaluate the effect of distance-to-finger, the DOE experiments (Supplementary information: Table 1) performed with paddle 3-30 were analysed separately. A positive effect of distance-to-probe on the stdev at different wavelengths was observed. The factor effect plot (Figure 6) displays the predicted stdev, and the confidence intervals of these predictions, at a specific wavelength (1300 nm) when the distance-to-finger is varied. The fact that 3 mm measurements resulted in higher stdev values could be attributed to a varying sample presentation caused by powder wave behaviour inside the feed frame triggered by paddle movement. Based on these results, it was decided to further use the 3-30 paddle wheel, an intermediate paddle speed of 60-80 rpm and 2 mm as distance-to-finger as parameters to develop models for in-line API monitoring. A distance-to-finger of 2 mm was chosen instead of 1 mm, since this set-up can then later still be compared to 2-16 paddle, where it is impossible to use 1 mm and since the difference in effect of 1 mm and 2 mm was small (considering the confidence intervals of the effects in Figure 6).

3.1.3 *Effect of filling degree on the NIR spectra*

The NIR spectra were clearly influenced by the filling degree of the feed frame. The spectra collected at the start-up phase did clearly differ from the other spectra (first eight spectra acquired, red spectra in Figure 7). In this period, the feed frame was empty, resulting in high absorbance spectra caused by the fact that nothing was measured and/or the highly absorbing material of the feed frame. During the filling of the feed frame, a clear trend in the spectra was visible (blue spectra 9 to 13 in Figure 7) the absorbance signal in the spectra was decreasing while filling the feed frame (green spectra 14 to 40 in Figure 7). Once the feed frame was filled, the spectral absorbance was constant (black spectra 41 to 100 in Figure 7).

The decrease in absorbance signal could be caused by the higher filling degree of the feed frame, resulting in a lower distance to probe, resulting in a higher reflectance. Another explanation of the decreasing absorbance could be the filling of the feed frame with powder blend, having a less absorbing character. At last, denser packing of material underneath the probe will cause less scattering, leading to an increase in reflection. Similar observations were made by Mateo-Ortiz et al.[1].

3.1. Development and validation of in-line NIR model for API content monitoring

3.2.1 *Validation of the in-line calibration models*

The saccharine concentrations of the validation set were predicted by means of the four developed models. Both, the individual predictions and the average of five predictions were used to analyse the performance of the individual models (15 predictions versus 3 predictions per repetition).

RMSEP was calculated for each concentration model (Table 4) and ranged from 0.1 to 1.7%. However, low RMSEP values do not guarantee that the results will be of adequate quality and reliability during future use. [22]. To asses predictive performance of the model in the future and to determine the concentration range over which the method will provide results of acceptable accuracy in the future, accuracy profiles were used.

For each validation concentration level, accuracy, precision and β-expectation tolerance intervals were calculated (Supplementary Information: Table 3 and Table 4). Both, relative bias and recovery stayed the same if the individual predictions or the averaged predictions (n=5) were used for the determination of the concentration. The repeatability (per day) and intermediate precision (between days) were lower for the 20% (w/w) predictions than for the 5% (w/w) predictions. β-expectation tolerance intervals became smaller when the predictions were based on the average of five predictions (5pred). This could be attributed to the smaller variance between the predicted values when average values were used.

In general, it was observed that PLS based models (model 1 and 2) performed better than ratio models (model 3 and 4). This could be explained by the fact that for the development of the PLS models, variables (wavelengths) are reduced to PLS components, excluding possible noise in the spectral data, and hence lowering the model error.

Accuracy profiles based on the average of five predictions (5pred) showed smaller β-expectation tolerance intervals. This could be explained by the fact that aberrant predictions were smoothened by averaging.

When model 1 and 2 for the 5% (w/w) predictions were used, future measurements would, with a probability of 95% fall outside the acceptance limits. For the concentration range of 4.5%-6.5%, both, model 1 and 2, were able to predict the true concentrations with a maximal total error of 15% (Figure 8). In general, the β-expectations tolerance intervals were wider at low concentrations. This could be explained by the fact that the relative total bias was plotted. An absolute bias of 0.8% on a 3.5% target concentration results in a relative bias of 23%, while on a 6.5% target concentration, the same absolute bias resulted in a relative bias of 12%. A consistent overprediction of the concentration at 3.5% target concentration was observed. This could be explained by the fact that 3.5% is a low concentration and the model is not able to predict lower concentrations, resulting in a higher amount of positive relative biases. Model 3 was rejected since the tolerance intervals ranged up to almost 60%.

When model 4 was used, the tolerance intervals were narrower, but still reached values up to 27% (Supplementary Information: Table 3).

Similarly to the analysis of the models for 5% (w/w), the performance of the models for 20% (w/w) was analysed. When model 1 was used, future measurements would, with a probability of 95% fall inside the limits of 15%. When model 2 was used, the tolerance intervals ranged up to almost 20%. Model 3 was also the poorest model for prediction of 20% (w/w) API as the largest tolerance intervals were obtained. When model 3 and model 4 were used, tolerance intervals ranged up to respectively 22.5% and 20% (Supplementary Information: Table 4).

Linearity of the model was assessed by regressing the predicted concentrations against the real (known) concentrations. The regression coefficient (R^2), slope and intercept were calculated (Table 4). An R^2 close to 1, a slope close to 1 and an intercept close to 0 suggest a good linear correlation. When the predictions were based on the average of five predictions, the R^2 value did increase remarkably. For 5% (w/w) concentration predictions, PLS models had a higher R^2 value compared to ratio models. Model 2 showed the best linear fit and best predictive performance based on accuracy profiles.

For 20% (w/w) concentration predictions, based on accuracy profiles, model 1 showed the best predictive performance. Model 1 and 4 were chosen as best PLS and ratio models, respectively.

3.3 Effect of paddle type, paddle speed and tableting speed on predictive performance

To evaluate the effect of paddle type, paddle speed and tableting speed on the predictive performance, the best PLS model and ratio model, according to the accuracy profiles, were evaluated (model 1 and 4, respectively).

Based on the NIR spectra acquired during runs with different paddle type, paddle speed and tableting speed (Table 3), the saccharine concentration of the 20% (w/w) formulation (based on 5 spectra) was predicted by model 1 and model 4.

Experiments 0-0 and 10-20 resulted in the largest variation in predicted concentrations, especially when model 4 was used, reflected by the standard deviation of the predictions (Table 5, experimental conditions explained in Table 3). The large variance in the predictions, when the original paddle wheel (0-0) was used, was caused by the paddle wheel fingers disturbances in the NIR spectra. No influence of the turret speed on the variability of the predictions was observed (experiment “250”, “3-30” and “750”). Finally, a paddle speed of 10-20 rpm caused more variation, while a paddle speed of 110-140 rpm caused less variation in the predictions. This could be due to the consistency of sample presentation (flow behaviour inside the feed frame).

While the standard deviation characterises the precision of the predictions, the accuracy of the predictions was represented by the RMSEP value of the predictions. Low RMSEP values were obtained for most experiments, except for experiments 0-0 and 10-20 as during these experiments paddles without notches and a low paddle speed were used, respectively.

4 Conclusion

In this work, an in-line NIR method with high speed acquisition of NIR spectra to allow real-time release (RTR) was developed for use in the feed frame of a tablet press. The measurement set-up was optimised by cutting notches inside the paddle wheel fingers. Cutting a notch with a width of 10 mm and a depth of 1 mm was sufficient to remove spectral disturbances caused by the moving paddle wheel. In this way, no pre-processing will be needed when physical characteristics of the powder blend such as density in the feed frame need to be studied.

In-line NIR spectroscopic methods were developed and evaluated using accuracy profiles for the monitoring of API concentration of a powder blend, with target concentration around 5% and 20% (w/w), in the feed frame during a tableting process. PLS models had a better predictive performance than ratio models, based on the accuracy profiles. A PLS model for the 5% (w/w) concentration was able to predict future concentrations with a maximal total error of 22.5% inside the range of 3.5 to 6.5% (w/w). If the model was used inside the range of 4.5 to 6.5% (w/w), the model was able to make predictions with a maximal total error of 15%. The model for 20% was able to make predictions of concentrations with a maximal total error of 15%.

The influence of several process parameters on predictive performance of models for 20% (w/w) API target concentration was investigated. Tableting speed did not influence the predictive performance. A lower paddle speed caused more variation in the acquired predictions, which could be caused by the fact that a lower sample size was measured when a lower paddle speed was applied. At a higher paddle speed, more powder passes underneath the probe during NIR acquisition, resulting in a larger sample size.

This set-up provides the opportunity for direct, in-line control of API concentration (and later feeding and segregation) inside the feed frame of the tablet press. When coupled with existing tablet press control systems and knowledge about the residence time distribution inside the feed frame, which is

493 indispensable for feedback and feedforward control, this method represents an important step
494 towards RTRt and RTR.

495 5 Acknowledgement

496 The authors would like to acknowledge GEA Pharma Systems™ (Halle, Belgium) for offering the
497 customised paddle wheel.

498

4. References

[1] D. Mateo-Ortiz, Y. Colon, R.J. Romañach, R. Méndez, Analysis of powder phenomena inside a Fette 3090 feed frame using in-line NIR spectroscopy, J. Pharm. Biomed. Anal. 100 (2014) 40–49.

[2] European Medicines Agency, Guideline on Real Time Release Testing (formerly Guideline on Parametric Release), 2012.

[3] P.R. Wahl, G. Fruhmann, S. Sacher, G. Straka, S. Sowinski, J.G. Khinast, PAT for tableting: Inline monitoring of API and excipients via NIR spectroscopy, Eur. J. Pharm. Biopharm. 87 (2014) 271–278.

[4] W. Li, A. Bashai-Woldu, J. Ballard, M. Johnson, M. Agresta, H. Rasmussen, S. Hu, J. Cunningham, D. Winstead, Applications of NIR in early stage formulation development. Part I. Semi-quantitative blend uniformity and content uniformity analyses by reflectance NIR without calibration models, Int. J. Pharm. 340 (2007) 97–103.

[5] W. Li, L. Bagnol, M. Berman, R.A. Chiarella, M. Gerber, Applications of NIR in early stage formulation development. Part II. Content uniformity evaluation of low dose tablets by principal component analysis, Int. J. Pharm. 380 (2009) 49–54.

[6] J. Gottfries, H. Depui, M. Fransson, M. Jongeneelen, M. Josefson, F.W. Langkilde, D.T. Witte, Vibrational spectrometry for the assessment of active substance in metoprolol tablets: A comparison between transmission and diffuse reflectance near-infrared spectrometry, J. Pharm. Biomed. Anal. 14 (1996) 1495–1503.

[7] M. Blanco, M. Alcalá, Content uniformity and tablet hardness testing of intact pharmaceutical tablets by near infrared spectroscopy: A contribution to process analytical technologies, Anal. Chim. Acta. 557 (2006) 353–359.

[8] E. Peeters, A.F. Tavares da Silva, M. Toiviainen, J. Van Renterghem, J. Vercruysse, M. Juuti, J.A. Lopes, T. De Beer, C. Vervaet, J.-P. Remon, Assessment and prediction of tablet properties using transmission and backscattering raman spectroscopy and transmission NIR spectroscopy, Asian J. Pharm. Sci. 11 (2016) 547–558.

[9] K. Järvinen, W. Hoehe, M. Järvinen, S. Poutiainen, M. Juuti, S. Borchert, In-line monitoring of the drug content of powder mixtures and tablets by near-infrared spectroscopy during the

528 continuous direct compression tableting process, Eur. J. Pharm. Sci. 48 (2013) 680–688.

529 [10] B. Bakri, M. Weimer, G. Hauck, G. Reich, Assessment of powder blend uniformity: Comparison
530 of real-time NIR blend monitoring with stratified sampling in combination with HPLC and at-line
531 NIR Chemical Imaging., Eur. J. Pharm. Biopharm. 97 (2015) 78–89.

532 [11] R.P. Cogdill, C. a Anderson, M. Delgado, R. Chisholm, R. Bolton, T. Herkert, A.M. Afnan, J.K.
533 Drennen, Process Analytical Technology Case Study Part I: Feasibility Studies for Quantitative
534 Near-Infrared Method Development, AAPS Pharmsci. 6 (2005) E262–E272.

535 [12] A.D. Karande, P.W.S. Heng, C.V. Liew, In-line quantification of micronized drug and excipients
536 in tablets by near infrared (NIR) spectroscopy: Real time monitoring of tabletting process, Int.
537 J. Pharm. 396 (2010) 63–74.

538 [13] Y. Liu, D. Blackwood, Sample Presentation in Rotary Tablet Press Feed Frame Monitoring by
539 Near Infrared Spectroscopy, Am. Pharm. Rev. (2012) 1–9.

540 [14] H.W. Ward, D.O. Blackwood, M. Polizzi, H. Clarke, Monitoring blend potency in a tablet press
541 feed frame using near infrared spectroscopy, J. Pharm. Biomed. Anal. 80 (2013) 18–23.

542 [15] R.J. Barnes, M.S. Dhanoa, S.J. Lister, Standard normal variate transformation and de-trending
543 of near-infrared diffuse reflectance spectra, Appl. Spectrosc. 43 (1989) 772–777.

544 [16] P. Hubert, J.J. Nguyen-Huu, B. Boulanger, E. Chapuzet, P. Chiap, N. Cohen, P. a. Compagnon, W.
545 Dewé, M. Feinberg, M. Lallier, M. Laurentie, N. Mercier, G. Muzard, C. Nivet, L. Valat,
546 Harmonization of strategies for the validation of quantitative analytical procedures: A SFSTP
547 proposal–Part III, J. Pharm. Biomed. Anal. 45 (2007) 82–96.

548 [17] P. Hubert, J.J. Nguyen-Huu, B. Boulanger, E. Chapuzet, P. Chiap, N. Cohen, P. a. Compagnon, W.
549 Dewé, M. Feinberg, M. Lallier, M. Laurentie, N. Mercier, G. Muzard, C. Nivet, L. Valat,
550 Harmonization of strategies for the validation of quantitative analytical procedures: A SFSTP
551 proposal - Part I, J. Pharm. Biomed. Anal. 36 (2004) 579–586.

552 [18] P. Hubert, J.J. Nguyen-Huu, B. Boulanger, E. Chapuzet, P. Chiap, N. Cohen, P. a. Compagnon, W.
553 Dewé, M. Feinberg, M. Lallier, M. Laurentie, N. Mercier, G. Muzard, C. Nivet, L. Valat,
554 Harmonization of strategies for the validation of quantitative analytical procedures A SFSTP
555 proposal – Part II, J. Pharm. Biomed. Anal. 45 (2007) 70–81.

556 [19] E. Peeters, T. De Beer, C. Vervaet, J.-P. Remon, Reduction of tablet weight variability by
557 optimizing paddle speed in the forced feeder of a high-speed rotary tablet press., Drug Dev.

Ind. Pharm. 41 (2015) 530–9.

[20] U.S. Department of Health and Human Services, Development and Submission of Near Infrared Analytical Procedures: Guidance for Industry (Draft Guidance),(2015).

[21] L. Saerens, N. Segher, C. Vervaet, J.P. Remon, T. De Beer, Validation of an in-line Raman spectroscopic method for continuous active pharmaceutical ingredient quantification during pharmaceutical hot-melt extrusion, Anal. Chim. Acta. 806 (2014) 180–187.

[22] C. De Bleye, P.F. Chavez, J. Mantanus, R. Marini, P. Hubert, E. Rozet, E. Ziemons, Critical review of near-infrared spectroscopic methods validations in pharmaceutical applications, J. Pharm. Biomed. Anal. 69 (2012) 125–132.

[23] P. Jacobs, W. Dewé, a. Flament, M. Gibella, a. Ceccato, A new validation approach applied to the GC determination of impurities in organic solvents, J. Pharm. Biomed. Anal. 40 (2006) 294–304.

[24] V. Cuzuel, J. Dugay, J. Brunet, A. Rey, J. Vial, V. Pichon, P.-L. Carrette, Validation of a liquid chromatography tandem Mass spectrometry method for targeted degradation compounds of ethanolamine used in CO2 capture: Application to real samples, Oil Gas Sci. Technol. 69 (2014).

[25] R.W. Mee, \beta-expectation and \beta-content Tolerance Limits for Balanced One-Way ANOVA Random Model, Technometrics. 26 (1984) 251–254.

[26] T.R.M. De Beer, W.R.G. Baeyens, a. Vermeire, D. Broes, J.P. Remon, C. Vervaet, Raman spectroscopic method for the determination of medroxyprogesterone acetate in a pharmaceutical suspension: validation of quantifying abilities, uncertainty assessment and comparison with the high performance liquid chromatography reference method, Anal. Chim. Acta. 589 (2007) 192–199.

[27] D.H. Shewiyo, E. Kaale, P.G. Risha, B. Dejaegher, J. De Beer, J. Smeyers-Verbeke, Y. Vander Heyden, Accuracy profiles assessing the validity for routine use of high-performance thin-layer chromatographic assays for drug formulations, J. Chromatogr. A. 1293 (2013) 159–169.

[28] E. Rozet, P. Lebrun, J.-F. Michiels, P. Sondag, T. Scherder, B. Boulanger, Analytical Procedure Validation and the Quality by Design Paradigm, J. Biopharm. Stat. 25 (2014) 260–268.

5. Figures and tables

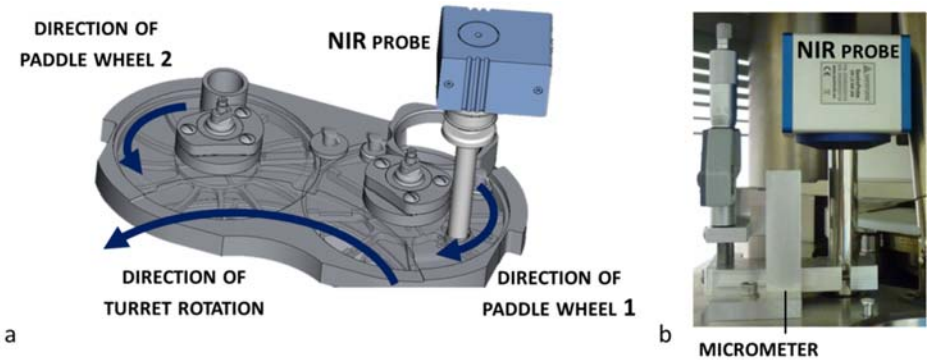

Figure 1 a. Location of the NIR spectrometer in the feed frame b. Micrometer with NIR probe

591 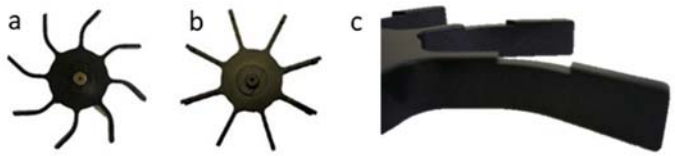

592 **Figure 2 a. Curved paddle wheel b. Straight paddle wheel c. Curved paddle wheel with notch**

593

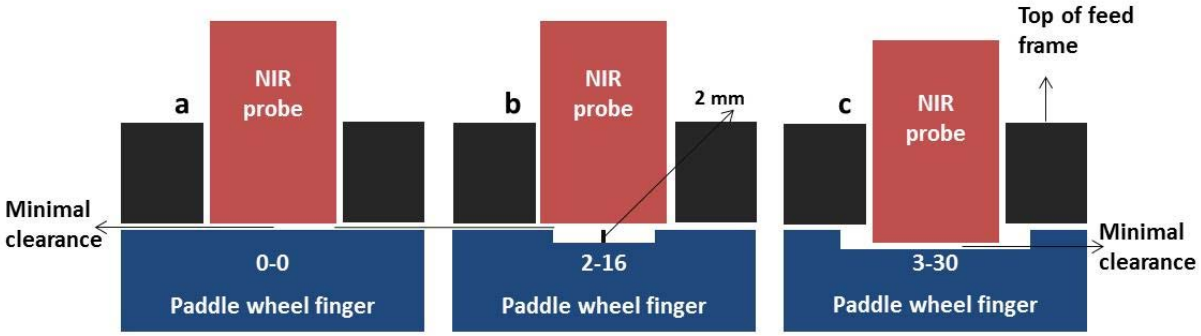

Figure 3 Visualisation of "base positions" of the NIR probe when using different paddle wheels, i.e. the lowest position possible to insert the probe inside the feed frame, without hindering the moving paddle wheel. When using 2-16, the distance between NIR probe (red) and paddle wheel (blue) in "base position" is 2 mm.

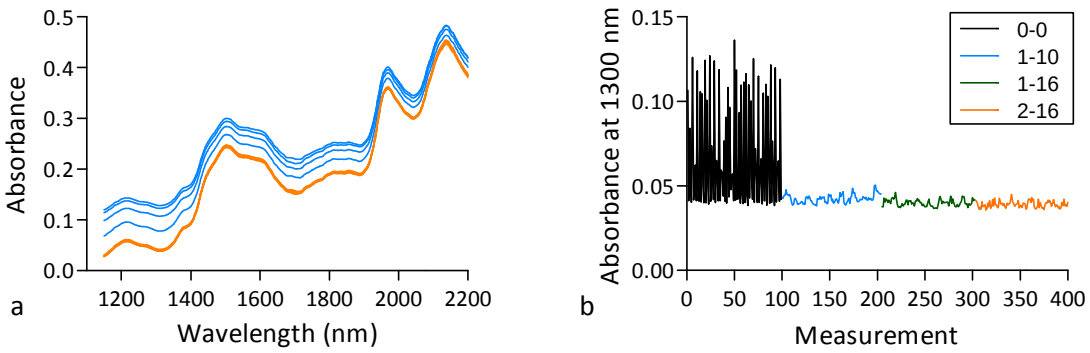

599

600 **Figure 4 a: NIR spectra acquired during tableting with disturbance caused by the moving paddle wheel (blue spectra).**
601 **b: Absorbance at 1300 nm, coloured according to different paddle wheel types.**

602

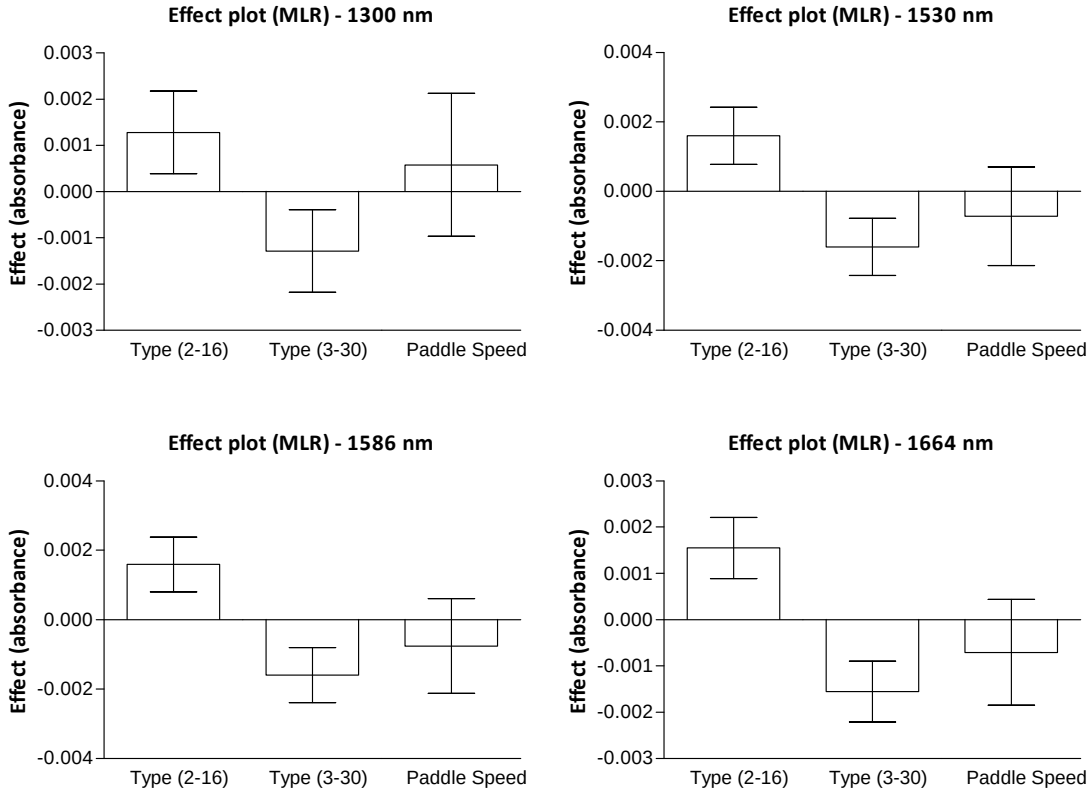

603

604 **Figure 5 The effect plots derived from the overall DOE showing the effect of paddle type and paddle speed upon stdev at**
605 **different wavelengths.**

606

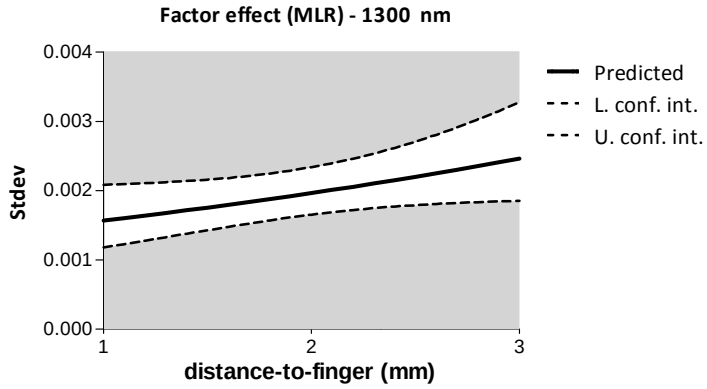

607

608 **Figure 6 DOE analysis performed with the 3-30 paddle. The factor effect displays the predicted values of stdev at**
609 **1300 nm, when the distance-to-finger varies over its range (1 - 3 mm) while all other factors in the design were set at**
610 **their average.**

611

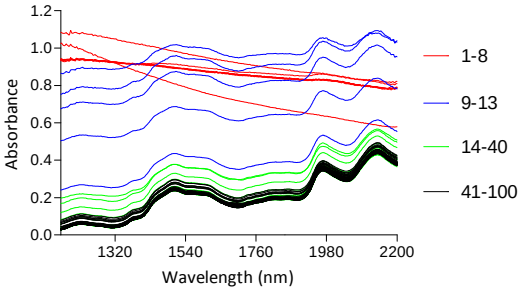

612

613 **Figure 7 Raw NIR spectra acquired during the start-up phase of the tableting process. Absorbance in function of**
614 **wavelength, coloured by number of collected spectra.**

615

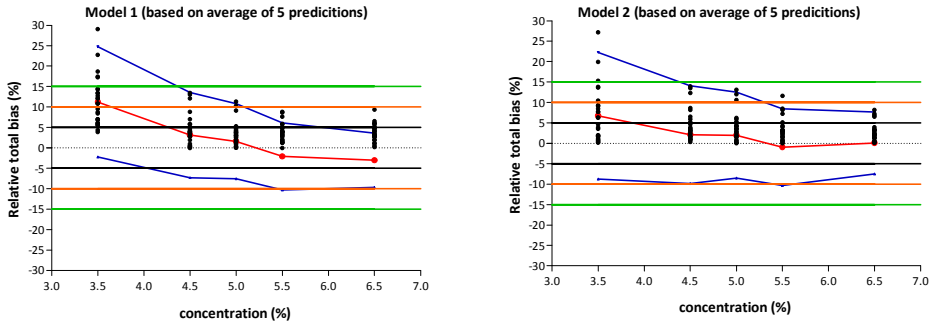

616

617 **Figure 8 Accuracy profiles of Model 1 and Model 2 for 5% (w/w) prediction. Black dots: relative total bias for each singe**
618 **measurement, red lines: mean total bias at each concentration, blue lines: β-expectation tolerance intervals, acceptance**
619 **limits of 5 (black), 10 (orange) and 15% (green).**

620

621

622 **Table 1 Compositions of formulations used**

Compound	Concentration (% w/w)	
Sodium Saccharine*	5.00	20.00
Avicel PH102**	30.33	25.33
Lactose**	60.67	50.67
Sodium Starch Glycolate	3.00	
Magnesium Stearate	1.00	

623 * the amount of sodium saccharine, MCC and lactose was varied during the experiments for API monitoring

624 **MCC- lactose ratio: 1:2

625

626

627 **Table 2 Composition of calibration (C) and validation (V) preblends for 5% (C5/V5) and 20% (C20/V20) (w/w)**

Blend: (in w/w%)	**C5-1**	**C5-2**	**C5-3**	**C5-4**	**C5-5**	**V5-1**	**V5-2**	**V5-3**	**V5-4**	**V5-5**
Sodium Saccharine	3	4	5	6	7	3.5	4.5	5	5.5	6.5
Avicel PH102	31.00	30.67	30.33	30.00	29.67	30.83	30.50	30.33	30.17	29.83
FastFlo Lactose	62.00	61.33	60.67	60.00	59.33	61.67	61.00	60.67	60.33	59.67
Magnesium Stearate	1	1	1	1	1	1	1	1	1	1
Sodium Starch Glycolate	3	3	3	3	3	3	3	3	3	3
Blend: (in w/w%)	**C20-1**	**C20-2**	**C20-3**	**C20-4**	**C20-5**	**V20-1**	**V20-2**	**V20-3**	**V20-4**	**V20-5**
Sodium Saccharine	15	17.5	20	22.5	25	16	18	20	22	24
Avicel PH102	27.00	26.17	25.33	24.50	23.67	26.67	26.00	25.33	24.67	24.00
FastFlo Lactose	54.00	52.33	50.67	49.00	47.33	53.33	52.00	50.67	49.33	48.00
Magnesium Stearate	1	1	1	1	1	1	1	1	1	1
Sodium Starch Glycolate	3	3	3	3	3	3	3	3	3	3

628

629

Table 3 Experiments performed to investigate the effect of paddle type, paddle speed and tableting speed on predictive performance of NIR model

Experiment	paddle type	paddle speed (rpm)	tableting speed (tpm)
0-0	0-0	60-80	500
2-16	2-16	60-80	500
250	3-30	60-80	250
750	3-30	60-80	750
10-20	3-30	10-20	500
110-140	3-30	110-140	500
3-30	3-30	60-80	500

634 **Table 4 RMSEP values and linearity test of the models for 5% and 20% predictions**

	RMSEP		R^2		Slope		Intercept	
5% (w/w)	1 pred	5 pred	1 pred	5 pred	1 pred	5 pred	1 pred	5 pred
Model 1	0.522	0.304	0.736	0.934	0.797	0.797	1.077	1.079
Model 2	0.560	0.272	0.736	0.934	0.915	0.915	0.500	0.019
Model 3	0.607	0.105	0.508	0.780	0.992		0.029	
Model 4	0.784	0.207	0.618	0.832	0.997		0.008	
20% (w/w)	1 spec	5 spec	1 spec	5 spec	1 spec	5 spec	1 spec	5 spec
Model 1	1.291	0.791	0.799	0.933	0.846	0.845	3.079	3.141
Model 2	1.452	0.843	0.761	0.919	0.866	0.867	2.498	2.528
Model 3	1.734	1.009	0.731	0.899	0.999		0.092	
Model 4	1.475	0.859	0.755	0.927	0.877		2.557	

635

636

637 **Table 5 Average prediction, stdev and RMSEP values of predictions made with model 1 and model 4, based on spectra**
638 **acquired during experiments presented in Table 3.**

Experiment	Average prediction (%)		stdev (%)		RMSEP (%)	
	Model 1	Model 4	Model 1	Model 4	Model 1	Model 4
0-0	19.5	18.9	0.4	1.1	0.6	1.5
2-16	20.2	19.9	0.3	0.6	0.3	0.5
3-30	20.2	20.1	0.5	0.6	0.5	0.6
250	20.4	20.1	0.3	0.6	0.5	0.6
750	20.1	20.0	0.4	0.7	0.4	0.7
10-20	20.5	20.8	0.7	1.3	0.8	1.5
110-140	20.0	19.8	0.2	0.5	0.2	0.5

639

640

641